Activation and characterization of Rb MEMS cells with an automatic system at wafer level

Sensors & Actuators: A. Physical 391 (2025) 116621

Contents lists available at ScienceDirect

Sensors and Actuators: A. Physical

journal homepage: www.journals.elsevier.com/sensors-and-actuators-a-physical

Activation and characterization of Rb MEMS cells with an automatic system at wafer level

M. Gozzelino [a],[1], E. Cerrato [a],[*],[1], C. Gionco [a], S. Micalizio [a], G. Aprile [a], M. Crivellari [b], F. Levi [a], D. Calonico [a]

[a] Quantum Metrology and Nanotechnologies Division, Istituto Nazionale di Ricerca Metrologica (INRIM), Strada delle Cacce 91, Torino, 10135, Italy
[b] Micro-nano Characterization and Fabrication Facility, Fondazione Bruno Kessler (FBK), Via Sommarive 18, 38123, Povo, Italy

ARTICLE INFO

Keywords:
Microcells
Silicon
Alkali
Rubidium

ABSTRACT

The push towards miniaturized and low-power quantum sensors demands reliable and mass-manufacturable atomic reservoirs. In this paper, we report on the implementation of an automatic system to activate and characterize a wafer of microfabricated Rb cells. The setup is composed of a motorized translation system jointly with two optical sources, a high-power one used for activating Rb pills and the other for spectroscopy purposes. The spectroscopy signal is analyzed in real-time to check the release of Rb during activation. Alternatively, the signal recognition can be used in post-production for screening the entire wafer. In this sense, the presented automated setup represents an effective tool to characterize the cell production in terms of Rb content and signal contrast, making a step towards mass production of devices based on miniaturized alkali vapor cells.

1. Introduction

Nowadays, microfabricated vapor-cells filled with alkali atoms represent the core component of a new generation of miniaturized quantum sensing devices, such as atomic clocks [1–4], magnetometers [5–8], gyroscopes [9] and electric field sensors based on Rydberg atoms [10]. In this regard, from the perspective of an ever-growing demand for small- size, low-power-consumption, and high-performance devices, the opportunity offered by MEMS-based technology in terms of hot atomic alkaline vapors confinement in cubic millimeters volumes (in vacuum or in presence of a buffer gas) is being leading to a fundamental breakthrough in the production of transportable frequency reference devices [3,11–13].

The main potential of MEMS-like microcells with respect to traditional glass-blown or cuvette vapor cells [14,15], is the high-level of integration with emerging photonic-integrated circuit platforms [16,17]. Such a significant enhancement would contribute to pivotal progresses in technological fields requiring stable and portable chip-scale atomic sensors, such as telecommunications, satellite positioning systems, avionics, biomedicine [5,18,19]. Moreover, the glass-blown approach notoriously suffers from poor reproducibility and large-scale production reliability [15], whereas micro-cell technology, inheriting established processes from the silicon industry, promises to make the cell production process more reproducible and scalable [20,21]. Indeed, in this case, hundreds of millimeter-size cells can be manufactured on a single wafer, within the same process run [22].

One of the main challenges for MEMS-cells production remains the yield and screening of the microcells, especially for what concerns the reproducibility, regardless of the alkaline metals filling method [23]. In this regard, the goodness of the microcells filling with alkali atoms needs to be validated and possibly quantified [24,25]. To make this technology appealing from an industrial point of view, it is then desirable to have a simple and cost-effective automated process monitoring the cells-filling process.

In this paper, we present an experimental setup that can automatically activate Rb dispensers with localized laser heating. The release of Rb can be monitored in real-time during the activation procedure, with the aim to increase the reproducibility of the filling process and to preserve the transparency of the cell windows. The same setup can also systematically perform a screening at wafer level, checking the presence of Rb vapor inside the microfabricated cells.

2. Setup description

The setup is composed of two main optical benches: one for the characterization of the sample and one serving as a reference (see Fig.

* Corresponding author.
E-mail address: e.cerrato@inrim.it (E. Cerrato).
[1] These authors contributed equally to this work.

https://doi.org/10.1016/j.sna.2025.116621
Received 22 January 2025; Received in revised form 3 April 2025; Accepted 22 April 2025
Available online 7 May 2025

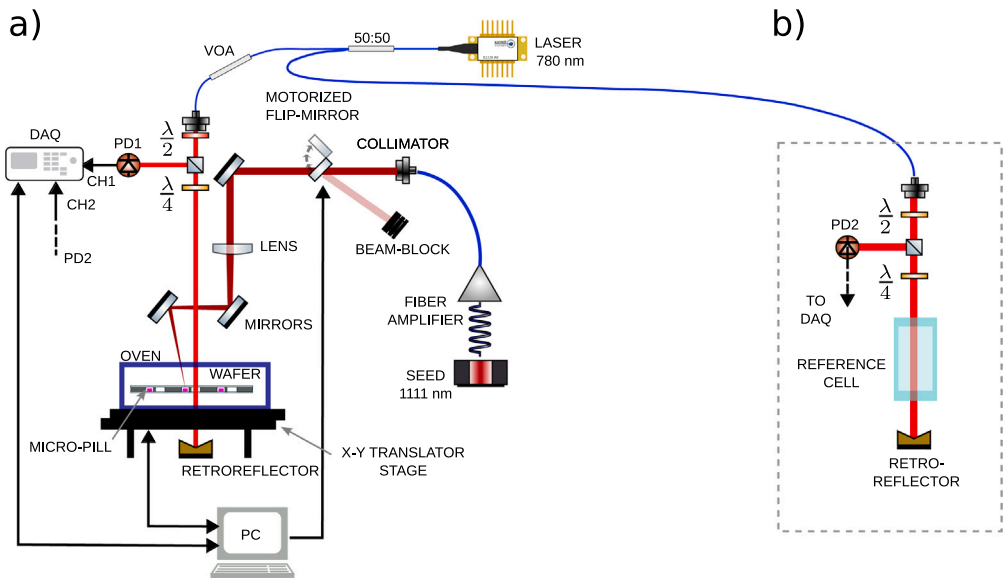

Fig. 1. (a) Scheme of the characterization setup. (b) Scheme of the reference setup. PD: photodiode, VOA: variable optical attenuator, DAQ: Digital acquisition system.

1(a) and 1(b), respectively). The reference bench contains a glass-blown cell filled with natural Rb. This cell has two purposes: first, it serves as a frequency reference to tune the spectroscopy laser in resonance with the Rb atoms. Secondly, it provides a benchmark absorption spectrum that can be compared to the signals coming from the devices under test. The characterization bench comprises the oven that can host silicon wafers up to 6 inches, a motorized translator stage and a two fixed laser heads for spectroscopy and laser activation of the Rb dispensers, respectively. Beam-shaping and collimation optics align the laser beams to the wafer. Along the free-space path of the activation laser, a motorized mechanical shutter regulates the amount of time the CW activation laser is sent to the wafer. The absorption signals are detected on a Silicon photodiode and acquired with a digital data acquisition system (DAQ). The synchronization between the DAQ, the translation stage and the optical shutter is provided with serial communication to a PC, that runs the acquisition software. The time needed for activation and translation of the wafer towards the next cell takes about 15 s, thus the time needed for activating the whole wafer can be as low as 1.5 h. Spectroscopy takes similar time (below 10 s per cell), thus the characterization can be done in about one hour. In the following subsections, the two setups are described in detail.

2.1. Spectroscopy setup

The oven consists of a central aluminum body that presents a circular ridge for holding a 6-inch wafer, that is then secured with the aid of two clamps. Smaller-diameter wafers or even single microcells can be mounted as well by means of suitable adapters. The base and the top covers are made of Delrin, an insulating material that has good stiffness and machinability. Two flanges allow the placement of two 15-cm optical windows, that are anti-reflection coated in the range from 600 nm to 1100 nm, allowing optical access on the Z axis. The oven is heated by 4 power resistors. The temperature setpoint can be regulated with a PID controller.

The oven is placed on top of a motorized X-Y translation stage. Three adjustable spacers allow for a small tilt of the oven, facilitating the alignment of the retroreflected beam, in case a reflecting coating is applied directly on the wafer back surface. The translation stage (Standa 8MTF-200) has a travel range of 200 mm by 200 mm, a minimum incremental motion of 0.65 µm and a repeatability of 0.5 µm. The stepper motor is controlled on the two axes with an encoder, which in turn is connected via USB to the control PC and is programmed with a Python software. The encoder is also equipped with a logic interface that is used to synchronize the movement of the oven with the acquisition of the spectroscopy signals.

The spectroscopy laser is a fiber-coupled distributed feedback (DFB) laser at 780 nm (Eagleyard DFB EYP-DFB-0780). The laser frequency setpoint is tuned to the Rb D_2 line by acting on the temperature and current setpoint. Frequency scanning across the line is performed with a triangular ramp on the laser current. The laser power is distributed into the main and into the reference benches with a 50:50 fiber splitter. A fiber variable optical attenuator regulates the laser power in the first case, whereas on the reference branch it can be regulated by rotating a half-waveplate just after the fiber launcher and filtering the light with a polarizing beam splitter.

The reference bench is composed of a fiber collimator (F810APC-780), of the aforementioned half-wave plate, of a polarizing beam splitter (PBS), of a 5-cm long quartz cell filled with isotopical Rb. A quarter-wave plate and a retroreflector create an optical circulator to implement the pump-probe configuration, enabling sub-Doppler spectroscopy. At the exit of the PBS, an amplified silicon photodiode (PD2) detects the retro-reflected light that circulates within the absorption cell (see Fig. 1(b)). The reference cell is heated close to room temperature, in order to have similar optical depth to the much shorter microcells that typically are heated above 60 °C.

The characterization bench follows the same absorption spectroscopy scheme. Here, the beam diameter is reduced to 1.2 mm to cope with the much smaller dimensions of the microcells (fiber collimator Thorlabs PAF2-A4B). The optics are mounted vertically by means of four optical rails. In this way the beam is directed along the Z direction, whereas the wafer is mounted onto a translator on the (X,Y) plane where it can be moved to perform spectroscopy over its whole surface. The spectroscopy is performed in double pass, with the aid of a retroreflector placed below the wafer. Retroreflected power is measured on a Si photodiode (PD1). When low laser intensity is sent to the wafer, simple Doppler absorption is performed. By increasing the input power, sub-Doppler saturated-absorption spectroscopy can be performed on the MEMS cells. In this latter case, a filter might optionally be placed before the retroreflector to optimize the pump-probe configuration.

The signals coming from PD1 and PD2 are synchronously acquired on a multichannel fast digital acquisition system (Keysight DAQ970 + DAQM909A) with 24 bit vertical resolution and an acquisition speed of up to 400 kS/s. The acquisition is syncronized using two triggers, one synchronous with the triangular ramp that scans the laser frequency, the other with the translation stage "stop" signal, so that the measurement start is conditioned to the correct alignment of the wafer.

2.2. Activation setup

The activation setup is composed of a CW fiber laser at 1111 nm (Koheras Adjustik Y10), followed by an Yb fiber amplifier (Keopsys CYFA-PB). The CW power available out of the fiber can be regulated through the amplifier driving current and is up to 1.8 W. A fiber launcher, mounted on the vertical breadboard beside the spectroscopy bench, focuses the beam with a $1/e^2$ diameter of 1.7 mm. Following the collimator, a mirror is mounted on a motorized stage (Thorlabs MFF101/M) redirecting the beam onto a beam-blocker, acting as a controllable mechanical shutter. The motorized stage has a response time of 200 ms. With the mechanical shutter open, the beam is then directed and aligned towards the wafer by means of three mirrors mounted on adjustable mirror posts. The mirrors allow to align the activation beam so that the beam spot at the wafer location has an offset with respect to the spectroscopy beam exactly matching the distance between the dispensing and the spectroscopy areas of the microcells. A lens (focal length 250 mm) focuses the beam to a 200 μm $1/e^2$ beam diameter on the wafer plane. By this means, the available intensity at the dispenser is up to 1.2×10^8 W m^{-2}.

3. Automatic spectroscopy and cell-validation algorithm

The spectroscopy over the whole wafer is performed by applying translation steps to the X-Y translation stage matching the spacing of the microcells grid. To ensure that there is no mismatch between the reference system of the translator and the cells grid, a preliminary alignment of the spectroscopy beam is performed manually over two far-apart cells with known relative position on the grid. The two positions of the translator (X_0, Y_0, X_1, Y_1) and the known row/column data are inserted as input parameters of the control software. The software then calculates the correct command to be applied to the translator (X_s, Y_s) at each step of the scan.

After this preliminary calibration of the system, the laser is aligned to the first-cell coordinates and the wafer is scanned automatically in a "S-shaped" manner. When the translator motor stops at the *i*th cell position, it sends a trigger to the DAQ that then starts the acquisition. When the acquisition is terminated, a new translation is applied, aligning the spectroscopy beam to the following cell. This process is iterated until the whole cell grid is scanned. Given that the laser diameter is typically a factor of two smaller than the diameter of the microcells (see Section 4), and the accuracy of the translator is better than 100 μm, optimal alignment is maintained over the whole wafer scan.

The signal coming from photodiode PD1 is acquired on one channel of the DAQ. On a second channel, the signal coming from the reference cell (PD2) is acquired at the same time. At the end of the acquisition, the data are downloaded to the PC and pre-processed. In particular, the signals are detrended after being normalized to the mean baseline intensity, to obtain the relative transmission free from amplitude modulation. Then, the processed signal coming from PD2 is compared to the one from the reference setup, to check the presence of Rb inside the microcell. The recognition of the Rb dips is obtained calculating the cross-correlation between the two signals (x and y) with the following formula:

$$R_{xy}[k] = \sum_{l=0}^{N-1} x_l \, y_{l-k+N-1}$$

where k is the index running over the data points acquired by the DAQ over a single scan, and N is the total number of samples of the scan. To automatically infer if a true Rb absorption signal is detected on the microcell, the maximum of the cross-correlation R_{xy} sis then compared to a threshold value. In our case, we found that a threshold value around 0.1 is a good compromise for recognizing the spectra and minimizing the false positives.

The signal detection algorithm described above has a double utility. First, it can be used to perform a sanity check of the cells already filled with alkali metal throughout the wafer. Alternatively, it can be used as a monitor for detecting the presence of Rb vapor during the activation of the alkali dispensers, and trigger the shutter on the high-power laser. The latter real-time monitoring of Rb release could be useful in the case of rapid diffusion of the Rb vapors, such in the case of communicating optical and dispensing cavities.

4. Experimental demonstration

4.1. MEMS-like microcell design and fabrication

In this section, the Rb-vapor MEMS-like microcell fabrication and design details are described. The Rb filling was carried out pursuing the dispensing-pills method [26]. The pills were purchased from SAES Getters. They are constituted by a Zr-Al alloy loaded with an alkali metal molybdate, containing an average Rb contempt of 0.4 mg. Six inches, 1 mm thick silicon wafer, was employed. The borosilicate glass wafer are 6 inches in diameter and 500-μm thick.

The wafer design, observable in Fig. 2(a), is constituted of 386 microcells homogeneously distributed on the wafer surface except for the two region in the middle of the wafer that correspond to the camera access holes of the anodic bonding machine and are dedicated to *in-situ* alignment. Each microcell is composed by a pair of connected passing cavities obtained in Si wafer. [26–28]. The smaller cavity, with a diameter of 1.5 mm, is named "dispensing cavity" and it is devoted to pills dispensing. The bigger one, with a diameter of 2 mm, is dedicated to the released Rb spectroscopy and it is called "optical cavity", as reported in Fig. 2(c). The two cavities are separated by 0.2 mm, and are connected by a passing channel with a width of 0.4 mm. The entire microcell size is 4.3 x 7.3 mm, including 0.15 mm on each side for the final microcell sawing.

The passing cavities in Si wafer are generated by means Deep Reactive Ion Etching (DRIE) process [28]. They are hermetically closed via anodic bonding on both sides, thus sealing the borosilicate wafers to silicon wafer and generating the 3D glass-silicon-glass structure.

The placement of the dispensing-pills is follows these steps: a first anodic bonding is made between the bottom glass and the perforated silicon wafer, producing what is usually called as "preform". Then, the pills are dropped in the dispensing cavities previous of the second anodic bonding. During the anodic bonding procedures, the wafer-bonder chamber is evacuated at 2×10^{-6} mbar, ensuring an environment free of moisture and water for the optimize performance of the microcells, preventing metal oxidation. The two plates are put in contact with a force of 700 N, heated at 350 °C and a voltage of 800 V is provided. A picture of the final realized wafer is reported in Fig. 2(b).

4.2. Wafer characterization

In this section, we present a few examples of activation and characterization of Rb MEMS cells at wafer level. Fig. 3 shows typical absorption spectra obtained with the setup described in Section 2. The data were recorded a few weeks after activation. The temperature of the oven was stabilized at 78 °C and the probe intensity was about 1 mW cm^{-2}. Specifically, the plot shows the result of a scan of 11 cells that were activated in the same activation run and with the same experimental conditions. In particular, the activation-laser power was 1.4 W and exposure time was determined on the basis of the observed spectroscopic signal (see Section 3). The correlation threshold was set to a value of 0.16. In Fig. 3, each scan is the result of a single laser frequency-ramp spanning several GHz, with 2000 points for the whole frequency range.

The activated cells present some degree of variability in the transmission, hence in the saturated Rb-vapor density. Nevertheless, thanks to the signal-driven activation, this variability is constrained to a standard deviation of 24 %. In this calculation we excluded 3 cells that initially provided the same level of absorption, that however almost

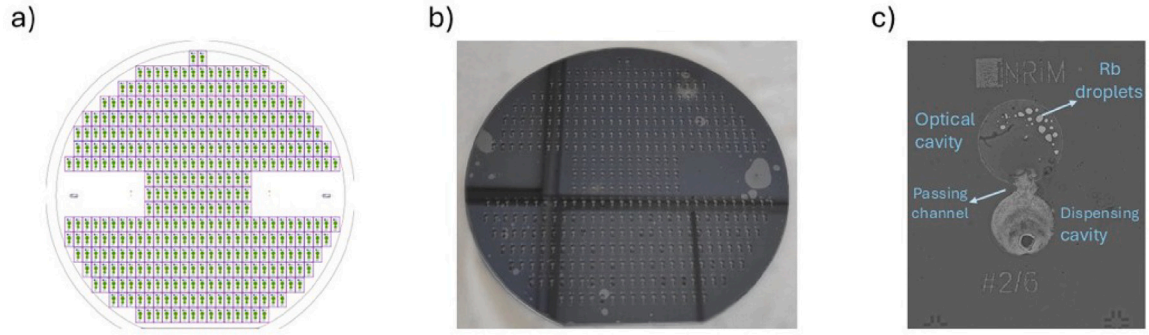

Fig. 2. (a) Wafer design scheme. (b) Picture of the realized wafer. (c) Picture of an activated microcell.

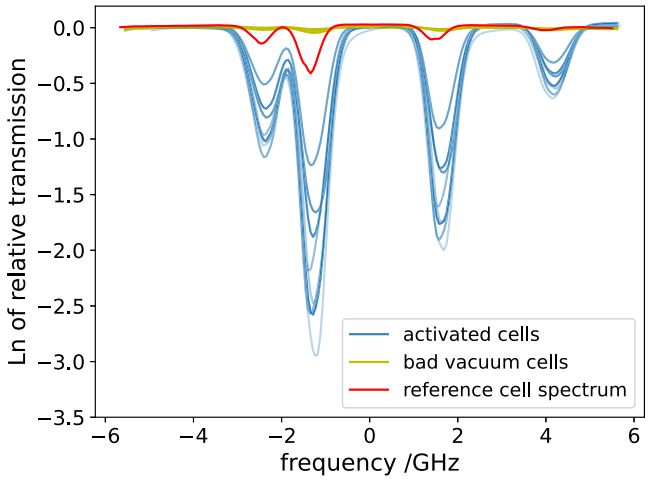

Fig. 3. Example of obtained transmission spectra for a scan of 11 cells (at a temperature of 78 °C). The *y*-axis is the natural logarithm of the relative absorption. In red, we compare the typical signal obtained on the reference cell. In red, we compare the typical signal obtained on the reference cell. (For interpretation of the references to color in this figure legend, the reader is referred to the web version of this article.)

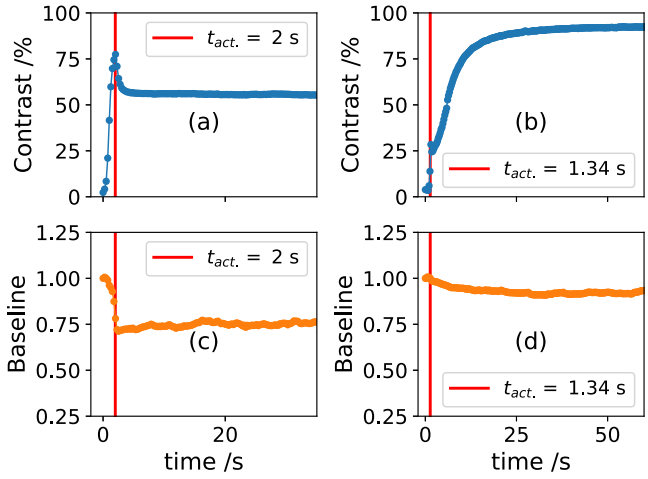

Fig. 4. (a) Contrast of the Rb-85 $F = 3 \rightarrow F' = 2, 3, 4$ Doppler-broadened profile during and after activation, for a cell activated at fixed time (2 s) and 1.4 W of laser power. (c) Out-of-resonance relative optical transmission (in double passage) through the optical cavity during and after activation for the same cell. (b) and (d) Contrast and relative transmission respectively, for a cell activated with the shutter driven by the spectroscopy signal (correlation threshold: 0.16). In all plots the activation starts at$t = 0$ and ends at the vertical red line. (For interpretation of the references to color in this figure legend, the reader is referred to the web version of this article.)

vanished over few hours (yellow traces in Fig. 3). We attribute the strong reduction of Rb signals to localized poorer vacuum levels inside the wafer in these cases, possibly due to not perfect hermeticity of the Si-glass anodic bonding.

Finally, we compare the two laser-activation methods for the Rb dispensers that are available with the described setup. The first activation procedure foresees a fixed activation time, whereas the second method foresees closing the shutter once a significant absorption signal is detected on the optical cell. The closing of the shutter in this case is performed when the correlation of the absorption signal with the reference profile exceeds a certain threshold. The latter method is interesting for improving the repeatability of the activation process and avoiding an excess of Rb deposition on the windows of the optical cavity. Fig. 4 shows two typical examples of activation with the two methods. As figures of merit, we analyzed the optical transmission (with the laser out of resonance) and the contrast of the absorption signals. Specifically, we calculated the contrast of the ^{85}Rb $F = 3 \rightarrow F' = 2, 3, 4$ Doppler-broadened profile. The transmission gives information about the cleanliness of the optical window during and after the activation. On the other hand, the contrast of the Rb lines is linked to the atomic density in the vapor phase in the weak probing regime. In Fig. 4(a) and (c), we observe the behavior of the spectroscopic signals and of the transmission for a cell activated with an intensity of 8.9×10^7 W m^{-2} and a fixed activation time of 2 s. We can observe that the absorption increases then settles to a lower value once the shutter is closed. On the other hand, the window transparency out of resonance decreases by 28 %. The settling can be interpreted by a temporary overheating of the cell due to the high power laser, whereas the loss in transparency of the optical windows is attributed to the deposition of metallic Rb on the windows, causing reflection and scattering. In the plots on the right, we show a typical transient observed when the shutter is closed after the correlation of the observed signal with the reference profile reaches a certain threshold (in this case 0.16). Here, the shutter is closed in a phase where the atomic absorption is still increasing (thus the release and equilibration of the Rb vapor inside the optical cavity is still ongoing). This is evident looking at the contrast of the Rb lines in Fig. 4(b). This method has proven to be advantageous also in preserving the transparency of the optical cavity that is typically maintained within 5 % (see Fig. 4(d)). We note that the rapid emergence of the spectroscopic signals is attributed to the relatively large passing channel between the dispensing cavity and the optical cavity.

5. Conclusions

The setup described in this work provides a convenient tool for activation and optical characterization of MEMS-like cells filled with Rb metals. Straightforward modifications can adapt the setup to work with Cs atoms as well. The setup is able to scan a whole 6-inches wafer in less than one hour, after a one-time manual alignment on the first

cell. Further improvements in the software could also make this pre-alignment procedure automatic, leading to a fully automated operation. The setup is also able to activate the Rb cell with the use of a high-power laser for localized heating of the Rb dispensers. Also in this case the procedure is automatic and the time for activation of a whole 6-inch wafer is less than two hours.

The importance of having a reliable testing equipment is demonstrated by the first analysis of the produced MEMS cell, that where characterized in terms of absorption. Increasing the statistics over more the whole wafer area and across multiple production batches is straightforward with the developed system and will be the basis of future work, where information about the quality and reproducibility of the wafer fabrication will be extracted.

In this work, we also demonstrate the convenience of simultaneous probing of the optical absorption during laser activation of the dispensers. This feature can either be used for performing a systematic study and tune the activation parameters or for the activation itself, conditioning the activation time to the absorption spectroscopy. The latter case has proven particularly useful in our case to avoid excess deposition of Rb droplets on the optical windows, preserving their transparency. The proposed setup marks an advancement in terms of reliable and large-scale production of high-quality vapor cells for the next-generation of atomic sensors based on Rb atoms.

CRediT authorship contribution statement

M. Gozzelino: Writing – review & editing, Writing – original draft, Visualization, Methodology, Investigation, Formal analysis, Data curation. **E. Cerrato:** Writing – review & editing, Writing – original draft, Investigation, Funding acquisition. **C. Gionco:** Visualization, Validation, Supervision, Project administration, Methodology, Funding acquisition, Conceptualization. **S. Micalizio:** Visualization, Supervision, Conceptualization. **G. Aprile:** Supervision, Funding acquisition. **M. Crivellari:** Methodology, Investigation, Conceptualization. **F. Levi:** Visualization, Validation, Conceptualization. **D. Calonico:** Visualization, Validation, Supervision, Project administration, Funding acquisition, Conceptualization.

Declaration of competing interest

The authors declare that they have no known competing financial interests or personal relationships that could have appeared to influence the work reported in this paper.

Acknowledgments

This research activity has been financially supported by the European Union's Horizon Europe research and innovation programme under the Grant Agreement n. 101135931 (Project QUANTIFY). Furthermore, part of this work has been performed at PiQuET (Piemonte Quantum Enabling Technology) Cleanroom at INRiM financed by the POR FESR 2014–2020 Program of the Piedmont Region. This research activity was partially supported by the European Space Agency, France, under the NAVISP element 2 Programme, Project M.O.D.O. Multichannel Optical/Ocxo Disciplined Oscillator (Activity Code NAVISP-EL2-158). Finally, partial funding came from the Italian Ministry of University and Research (MUR) in the framework of the continuing-nature project "NEXT- GENERATION METROLOGY", under the allocation of the Ordinary Fund for research institutions (FOE) 2023 (Ministry Decree n. 789/2023).

Data availability

Data will be made available on request.

References

[1] J. Kitching, Chip-scale atomic devices, Appl. Phys. Rev. 5 (3) (2018) 031302, http://dx.doi.org/10.1063/1.5026238.

[2] E. Batori, C. Affolderbach, M. Pellaton, F. Gruet, M. Violetti, Y. Su, A.K. Skrivervik, G. Mileti, μPOP clock: A microcell atomic clock based on a double-resonance Ramsey scheme, Phys. Rev. Appl. 18 (5) (2022) 054039, http://dx.doi.org/10.1103/physrevapplied.18.054039.

[3] V. Maurice, Z.L. Newman, S. Dickerson, M. Rivers, J. Hsiao, P. Greene, M. Mescher, J. Kitching, M.T. Hummon, C. Johnson, Miniaturized optical frequency reference for next-generation portable optical clocks, Opt. Express 28 (17) (2020) 24708–24720, http://dx.doi.org/10.1364/OE.396296, URL https://opg.optica.org/oe/abstract.cfm?URI=oe-28-17-24708.

[4] S. Knappe, V. Shah, P.D.D. Schwindt, L. Hollberg, J. Kitching, L.-A. Liew, J. Moreland, A microfabricated atomic clock, Appl. Phys. Lett. 85 (9) (2004) 1460–1462.

[5] V. Shah, S. Knappe, P.D.D. Schwindt, J. Kitching, Subpicotesla atomic magnetometry with a microfabricated vapour cell, Nat. Photonics 1 (11) (2007) 649–652, http://dx.doi.org/10.1038/nphoton.2007.201.

[6] H. Raghavan, M.C. Tayler, K. Mouloudakis, R. Rae, S. Lähteenmäki, R. Zetter, P. Laine, J. Haesler, L. Balet, T. Overstolz, S. Karlen, M.W. Mitchell, Functionalized millimeter-scale vapor cells for alkali-metal spectroscopy and magnetometry, Phys. Rev. Appl. 22 (2024) 044011, http://dx.doi.org/10.1103/PhysRevApplied.22.044011, URL https://link.aps.org/doi/10.1103/PhysRevApplied.22.044011.

[7] E. Boto, N. Holmes, J. Leggett, G. Roberts, V. Shah, S. Meyer, L. Muñoz, K. Mullinger, T. Tierney, S. Bestmann, G. Barnes, R. Bowtell, M. Brookes, Moving magnetoencephalography towards real-world applications with a wearable system, Nature 555 (2018) 657–661, http://dx.doi.org/10.1038/nature26147.

[8] W.C. Griffith, S. Knappe, J. Kitching, Femtotesla atomic magnetometry in a microfabricated vapor cell, Opt. Express 18 (26) (2010) 27167–27172, http://dx.doi.org/10.1364/OE.18.027167, URL https://opg.optica.org/oe/abstract.cfm?URI=oe-18-26-27167.

[9] Y. Chen, M. Yu, Y. Ma, G. Luo, Z. Jiang, Y. Bai, L. Zhao, Micro-fabricated alkali vapor cells for atomic spin gyroscope study, in: 2021 IEEE 16th International Conference on Nano/Micro Engineered and Molecular Systems, NEMS, 2021, pp. 282–285, http://dx.doi.org/10.1109/NEMS51815.2021.9451404.

[10] J. Zhu, R. Zhao, Z. Li, D. Hao, K. Zu, Y. Shi, J. Tang, J. Liu, Development of a cesium vapor MEMS cell for differential measurement of microwave electromagnetically induced transparency, IEEE Electron Device Lett. 44 (1) (2023) 132–135, http://dx.doi.org/10.1109/LED.2022.3219922.

[11] Z.L. Newman, V. Maurice, C. Fredrick, T. Fortier, H. Leopardi, L. Hollberg, S.A. Diddams, J. Kitching, M.T. Hummon, High-performance, compact optical standard, Opt. Lett. 46 (18) (2021) 4702–4705.

[12] E. Klinger, A. Mursa, C.M. Rivera-Aguilar, R. Vicarini, N. Passilly, R. Boudot, Sub-Doppler spectroscopy of the Cs atom 6S1/2–7P1/2 transition at 459 nm in a microfabricated vapor cell, Opt. Lett. 49 (8) (2024) 1953, http://dx.doi.org/10.1364/ol.514866.

[13] M. Callejo, A. Mursa, R. Vicarini, E. Klinger, Q. Tanguy, J. Millo, N. Passilly, R. Boudot, Short-term stability of a microcell optical reference based on rb atom two-photon transition at 778 nm, 2024, http://dx.doi.org/10.48550/ARXIV.2407.00841.

[14] J. Vanier, C. Audoin, The Quantum Physics of Atomic Frequency Standards, Adam Hilger, Bristol, 1989.

[15] A. Godone, F. Levi, C. Calosso, S. Micalizio, High-performing vapor-cell frequency standards, Riv. Nuovo Cimento 38 (2015) 133–171, http://dx.doi.org/10.1393/ncr/i2015-10110-4.

[16] M.T. Hummon, S. Kang, D.G. Bopp, Q. Li, D.A. Westly, S. Kim, C. Fredrick, S.A. Diddams, K. Srinivasan, V. Aksyuk, J.E. Kitching, Photonic chip for laser stabilization to an atomic vapor with 10-11 instability, Optica 5 (4) (2018) 443–449, http://dx.doi.org/10.1364/OPTICA.5.000443, URL https://opg.optica.org/optica/abstract.cfm?URI=optica-5-4-443.

[17] A. Yulaev, C. Ropp, J. Kitching, V.A. Aksyuk, M.T. Hummon, Chip-scale sub-Doppler atomic spectroscopy enabled by a metasurface integrated photonic emitter, Appl. Phys. Lett. 125 (12) (2024) http://dx.doi.org/10.1063/5.0222456.

[18] M.V. Balabas, D. Budker, J. Kitching, P.D.D. Schwindt, J.E. Stalnaker, Magnetometry with millimeter-scale antirelaxation-coated alkali-metal vapor cells, J. Opt. Soc. Am. B 23 (6) (2006) 1001–1006, http://dx.doi.org/10.1364/JOSAB.23.001001, URL https://opg.optica.org/josab/abstract.cfm?URI=josab-23-6-1001.

[19] J. Fang, J. Qin, Advances in atomic gyroscopes: A view from inertial navigation applications, Sensors 12 (5) (2012) 6331–6346, http://dx.doi.org/10.3390/s120506331, URL https://www.mdpi.com/1424-8220/12/5/6331.

[20] L.-A. Liew, S. Knappe, J. Moreland, H. Robinson, L. Hollberg, J. Kitching, Microfabricated alkali atom vapor cells, Appl. Phys. Lett. 84 (14) (2004) 2694–2696, http://dx.doi.org/10.1063/1.1691490, arXiv:https://pubs.aip.org/aip/apl/article-pdf/84/14/2694/18587403/2694_1_online.pdf.

[21] T. Overstolz, J. Haesler, G. Bergonzi, A. Pezous, P.-A. Clerc, S. Ischer, J. Kaufmann, M. Despont, Wafer scale fabrication of highly integrated rubidium vapor cells, in: 2014 IEEE 27th International Conference on Micro Electro Mechanical Systems, MEMS, IEEE, 2014, http://dx.doi.org/10.1109/memsys.2014.6765700.

[22] R. Vicarini, V. Maurice, M. Abdel Hafiz, J. Rutkowski, C. Gorecki, N. Passilly, L. Ribetto, V. Gaff, V. Volant, S. Galliou, R. Boudot, Demonstration of the mass-producible feature of a Cs vapor microcell technology for miniature atomic clocks, Sensors Actuators A: Phys. 280 (2018) 99–106, http://dx.doi.org/10.1016/j.sna.2018.07.032, URL https://www.sciencedirect.com/science/article/pii/S0924424718305387.
[23] D.G. Bopp, V.M. Maurice, J.E. Kitching, Wafer-level fabrication of alkali vapor cells using in-situ atomic deposition, J. Phys.: Photonics 3 (1) (2020) 015002, http://dx.doi.org/10.1088/2515-7647/abcbe5.
[24] S. Karlen, J. Gobet, T. Overstolz, J. Haesler, S. Lecomte, Lifetime assessment of RbN3-filled MEMS atomic vapor cells with Al2O3 coating, Opt. Express 25 (3) (2017) 2187–2194, http://dx.doi.org/10.1364/OE.25.002187, URL https://opg.optica.org/oe/abstract.cfm?URI=oe-25-3-2187.
[25] V. Maurice, Design, microfabrication and characterization of alkali vapor cells for miniature atomic frequency references (Ph.D. thesis), Université de Franche-Comtè, 2016.
[26] L. Nieradko, C. Gorecki, J. Dziuban, A. Douahi, V. Giordano, J. Beugnot, S. Guerandel, M. Moraja, From the implementation to the characterisation and assembling of microfabricated optical alcali vapor cell for MEMS atomic clocks, in: TRANSDUCERS 2007 - 2007 International Solid-State Sensors, Actuators and Microsystems Conference, vol. 133, (214501) 2007, pp. 45–48, http://dx.doi.org/10.1109/SENSOR.2007.4300067.
[27] M. Hasegawa, R. Chutani, C. Gorecki, R. Boudot, P. Dziuban, V. Giordano, S. Clatot, L. Mauri, Microfabrication of cesium vapor cells with buffer gas for MEMS atomic clocks, Sensors Actuators A: Phys. 167 (2) (2011) 594–601, http://dx.doi.org/10.1016/j.sna.2011.02.039.
[28] C. Carlé, S. Keshavarzi, A. Mursa, P. Karvinen, R. Chutani, S. Bargiel, S. Queste, R. Vicarini, P. Abbé, M. Abdel Hafiz, V. Maurice, R. Boudot, N. Passilly, Reduction of helium permeation in microfabricated cells using aluminosilicate glass substrates and Al2O3 coatings, J. Appl. Phys. 133 (21) (2023) 214501.

Michele Gozzelino received his Master's degree in Physics from the University of Florence, Italy, in 2016. The same year he joined the Time and Frequency group of Istituto Nazionale di Ricerca Metrologica (INRIM), Turin, Italy. In 2018, he was visiting Ph.D. at ICFO (Barcelona, Spain), performing studies on squeezed light applied to magnetometry. He received the Ph.D. in Metrology from Politecnico di Torino in 2020 and is now working as a researcher at INRIM. His research interests include atomic spectroscopy, atomic clocks and laser physics.

Erik Cerrato received the Master in Material Science in 2016 at the chemistry department of the University of Turin, where he also obtained the Ph.D. in Chemistry and Material Science in 2019 defending the thesis titled "Innovative, oxide based, photoactive systems for photocatalytic applications and solar fuel production". He joined INRiM institute in 2021, as a senior post-doc in the time and frequency sector at the quantum metrology and nanotechnologies division. Since 2022 he got a permanent position as research technologist in the interdivisional research infrastructures sector, directly connected to cleanroom facility. His current major research interests are the microfabrication of alkali vapor cells for quantum sensing devices and the design and characterization of photonic chips, with a particular focus on micro-rings structures for optical comb generation.

Chiara Gionco is a materials scientist with expertise in the synthesis and characterization (mainly spectroscopical) of lanthanide doped oxides. Besides the academic experience, she worked for a couple of years in the microelectronics industry, where she acquired both hard (related to the assembly and packaging of devices) and soft (like project and time management in a fast-paced environment) skills. She joined the Italian Metrology Institute (INRiM) as a permanent researcher in 2020 and is involved in the miniaturization of optical clocks, within the Time and Frequency research group, and in parallel in the management of the PiQuET facility.

Salvatore Micalizio received the degree in physics from University of Turin. In 2002 he received the Ph.D. in metrology from the Politecnico of Turin. His research activity was devoted to the development of a maser based on the Coherent Population Trapping phenomenon. He is now with the Physics Metrology Division of the Istituto Nazionale di Ricerca Metrologica (INRIM) of Turin. His research activity is mainly devoted to theoretical studies of the physics of vapor-cell clocks. In particular, he contributed to the development of a rubidium maser based on the coherent population trapping (CPT) phenomenon and of a pulsed optically pumped (POP) clock. He was responsible of several contracts funded by the Italian Space Agency (ASI), by the European Space Agency (ESA) and by the European Metrological Research Program (EMRP).

Giulia Aprile earned her Master's degree in Industrial Chemistry from the University of Turin, Italy, in 2013, and her Ph.D. in Chemistry from the University of Piemonte Orientale, Vercelli, Italy, in 2017. She subsequently spent five years as a research fellow specializing in nano- and microfabrication. Currently, she works as a full-time technologist at INRiM, where she works for the miniaturization of optical clocks within the Time and Frequency research group. In addition, she manages the PiQuET Cleanroom and leads the Interdivisional Research Infrastructures working group.

Michele Crivellari is a researcher at the Sensors and Devices Center of the Fondazione Bruno Kessler (FBK) in Trento, Italy. Since 2001, he has specialized in micro-nano fabrication and characterization technologies, focusing on silicon-based MEMS devices, including flow sensors, gas sensors, and microfluidic systems. His expertise also extends to the hetero-integration of materials such as silicon carbide (SiC) and gallium arsenide (GaAs). From 2010 to 2023, Dr. Crivellari coordinated the MEMS fabrication area in the Micro-Nano Fabrication Facility (MNF) and now oversees its research activities, focusing on PVD and wafer bonding processes. He has collaborated with leading institutions worldwide and has authored or co-authored more than 60 publications in peer-reviewed journals and conference proceedings.

Filippo Levi received the master's degree in physics from the University of Turin, Turin, Italy, in 1992, and the Ph.D. degree in metrology from the Politecnico di Torino, Torino, in 1996.

Since 1995, he has been with the Istituto Nazionale di Ricerca Metrologica (INRIM), Torino, where he is currently a Research Director leading the time and frequency research activities. His main research interests include development of secondary and primary microwave and optical atomic frequency standards, as well as time and frequency reference dissemination. In 1998, and then again in 2004 and 2005, he was a Guest Researcher with the Time and Frequency Division at NIST, to study application of laser-cooling technique to atomic frequency standards.

Davide Calonico, physicist, Ph.D. in metrology from the Politecnico di Torino in 2003. Research Director at the Istituto Nazionale di Ricerca Metrologica (INRiM), he devoted his research activity to time and frequency metrology and to quantum technologies. Since 2019 is the responsible of the Research Infrastructure "Piemonte Quantum Enabling Technology (Piquet)", with a scientific focus on the development of quantum devices.